Model reduction for efficient FEM/BEM coupling

Gérald Kergourlay, Etienne Balmès, Didier Clouteau
Ecole Centrale Paris, MSSMat, 92295 Chatenay Malabry Cedex, France
kergourlay@mss.ecp.fr, balmes@mss.ecp.fr, clouteau@mss.ecp.fr

Abstract

Model reduction techniques seek approximate solutions of a problem with a large number of DOFs within a subspace of small dimension. Component Mode Synthesis (CMS) methods form a large class of reduction methods where the subspace is selected *a priori*. Introducing *a posteriori* error estimation and iterative correction significantly extends the range of applications of reduction methods. The paper focuses on possible uses of reduction methods for coupled Finite Element (FEM) / Boundary Element (BEM) predictions in cases where the boundary contains a significant number of Degrees Of Freedom (DOFs) and where the coupling significantly affects the response of the structure. Issues addressed, for the case of a reactor building, are error evaluations for the coupled responses when using a FEM model reduced *a priori* and performance evaluations when using an iterative scheme that guarantees a given level of error.

1. Introduction

Coupled Finite Element (FEM) / Boundary Element (BEM) models are often considered for fluid or soil structure interaction problems. In such problems, the FEM model is typically reduced using methods related to Component Mode Synthesis (CMS) [1]. The resulting model contains dynamic modes (free, fixed or loaded boundary conditions) and static responses to unit displacements or loads applied to all Degrees Of Freedom (DOFs) of the interface between the structure and the fluid/soil.

The present study focuses on soil/structure interaction problems, where the soil stiffness significantly affects the response of buildings, and cases where the soil/structure interface contains a significant number of DOFs. In such problems, evaluating the dynamic soil stiffness is obviously expensive, but just manipulating the associated large full complex matrices already requires significant resources.

The objective of the paper is to validate the use of generalized interface DOFs as a means to reduce computational costs. This problem is strongly related to the interface model reduction in CMS methods [2, 3, 4]. The novelty is to address error estimation and introduce iterative correction schemes.

Section 2. summarizes theoretical tools (model reduction, error estimation and singular value decomposition) used in the paper to analyze the performance of various reduction methods. An essential aspect of the proposed tools is the use of a reference elastic model to build *a priori* reduction basis, estimate errors and introduce iterative schemes leading to the exact solution.

Section 3. tests a number of interface reduction methods on the case of the soil/structure interaction of a nuclear reactor building excited by *sv*, *sh* (shear) and *p* (pressure) waves with different incidences. The objective of this numerical application is to show the ingredients that are needed to build methods that work well in all cases and illustrate the associated rates of convergence.

2. Model reduction tools

2.1 Reducing a discrete model

One here considers already discretized models, that can be described by an equation of the form

$$\begin{aligned} [Z(s)]_{N\times N}\{q(s)\} &= [b]_{N\times NA}\{u(s)\}_{NA\times 1} \\ \{y(s)\}_{NS\times 1} &= [c]_{NS\times N}\{q(s)\}_{N\times 1} \end{aligned} \tag{1}$$

where for a standard elastic model $Z = Ms^2 + K$ and for the current application the form is (10).

The idea of a displacement based approximation (Ritz analysis) is to seek the approximate answer within the subspace spanned by a projection basis described by the real matrix $[T]$ and associated with generalized DOFs $\{q_R\}$

$$\{q\} = [T]\{q_R\} \tag{2}$$

One further assumes that the equilibrium equations are projected on the basis dual to $[T]$ which leads to a model of the form

$$\begin{aligned} \left[T^T Z(s) T\right]_{NR\times NR}\{q_R\} &= \left[T^T b\right]\{u(s)\} \\ \{y(s)\}_{NS\times 1} &= [cT]_{NS\times NR}\{q_R(s)\}_{NR\times 1} \end{aligned} \tag{3}$$

The quality of the approximation is based on the fact that all effectively found states of $\{q\}$ are well approximated in the span of $[T]$. Methods are distinguished by the reference problems used to generate $[T]$. Standard CMS approaches [1] take into account

- the frequency content of the applied loads, and thus keep modes within the frequency range of interest.
- the spatial content of the applied loads, and thus keep static responses to a subspace of loads describing that content.

For problems where the stiffness is frequency dependent, standard CMS methods cannot be applied directly since computing modes becomes a problem. The method retained here is to use a single reference stiffness K_0 for energy evaluations and a static response operator K_d^{-1} to compute static responses.

K_0 must be representative of energy distribution in the structure. Taking the real part of the complex stiffness at a given frequency is usually efficient but other approaches can be considered. For soil-structure interaction a model with ground springs is efficient because there properties can be typically be estimated without calling the BEM code.

K_d^{-1} normally is the inverse of K_0. For free floating structures, this inverse does not exist, so that a mass shifted matrix or a pseudo-inverse of K_0 [5] is used.

2.2 Error estimation

For a given reduced solution, one can easily build a residue that is characteristic of the error. Thus for harmonic responses given by $\{q_R\} = \left[T^T Z(s,p) T\right]^{-1}\left[T^T b\right]\{u(s)\}$, the residue is the load

$$\{R_L(s,u)\} = [Z(s,p)]\,[T]\,\{q_r\} - [b]\,\{u(s)\} \tag{4}$$

To associate an energy with this load, one seeks the associated static response

$$\{R_D(s,u)\} = \left[K_d^{-1}\right]\{R_L\} \tag{5}$$

Note that the use of this particular response could be justified by the fact that it maximizes the ratio of work under R_L and energy of the considered displacement.

An estimate of the error in the sense of the strain energy is thus given by

$$e(s,u) = \frac{\{R_D(s,u)\}^T [K_0]\{R_D(s,u)\}}{\{q_R(s,u)\}^T [T^T K_0 T]\{q_R(s,u)\}} \tag{6}$$

While error estimation is first used to establish convergence of the approximation, it provides a natural mechanism [6] to correct the initial reduction basis by adding displacement residuals to the basis

$$[T_{i+1}] = [[T_i] \;\; \mathrm{Re}\,[R_D(\omega_k, u_k)] \;\; \mathrm{Im}\,[R_D]] \tag{7}$$

where a number of strategies can be defined to restrict the number of frequencies and loading cases (ω_k, u_k) used to build the refined basis.

2.3 Principal directions

When defining a reference problem to build a reduction basis, it often happens that its dimension is larger than really needed. Having a simple mechanism to select vectors within a basis is thus fundamental. The Singular Value Decomposition (SVD) is a major mathematical tool allowing the classification of directions within a subspace. The general form of the decomposition of a matrix $[T]$

$$[T]_{N\times NR} = [U]_{N\times N}\,[\Sigma]_{N\times NR}\,[V]^T_{NR\times NR} \tag{8}$$

where, Σ contains singular values on its diagonal, and U, V are orthonormal matrices of right left and right singular vectors.

Classical SVD uses Euclidian norms, but in mechanics, it makes more sense to use strain and kinetic energy norms. Thus, the principal displacements of a given subspace can be defined as stationary points of

$$J(q) = \frac{\{q\}^T [K]\{q\}}{\{q\}^T [M]\{q\}} \tag{9}$$

where one will recognize Rayleigh's quotient. Modal truncation is thus equivalent to a SVD where all unit kinetic energy displacements are considered equally probable and the most important directions are associated with small strain energies.

This generalization of the SVD (see other details in Ref. [7]) is important to justify the use of modal truncation for bases which need not be modal bases using norms that only need to be representative of the physics of the problem. Here the M and K_0 norms are used.

3. FEM/BEM applications

3.1 Numerical application

The proposed methodologies will be illustrated on the case of the seismic response of the building shown in figure 1.

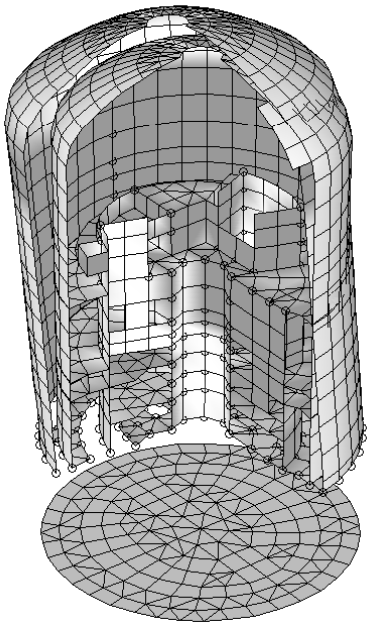

Figure 1: First fixed interface mode for the model of a Pressurized Water Reactor Building. The soil/structure interface is lowered for the plot.

The objective is to validate methodologies that can be used to approximate the response to incoming *sv, sh* (shear) and *p* (compression) waves with various incidences. In other words, solve a series of problems of the form

$$\left[\begin{array}{cc} Z_{II} + Z_{II,Soil} & Z_{IC} \\ Z_{CI} & Z_{CC} \end{array} \right] \left\{ \begin{array}{c} q_I \\ q_C \end{array} \right\} = \left\{ \begin{array}{c} F_I \\ 0 \end{array} \right\} \quad (10)$$

where, F_I describes the seismic loading and has a significant dependence on frequency, and $Z_{II,Soil}$ describes the soil impedance (built with the BEM) which is not negligible when compared to the building contribution Z_{II} (obtained with the FEM).

For structures with large foundations, the number of DOFs in the interface is quite high and BEM computational costs increase rapidly with the number of such DOFs. Thus, there is a strong interest in not only reducing internal structure DOFs q_C (which would be classical CMS) but also interface DOFs q_I.

Here, the soil impedance is obtained from MISS3D by mean of a BEM for a layered soil [8, 9]. The building model, a Craig-Bampton reduction of the initial building model, is exported from ASTER [10, 11]. This model contains 558 interface DOFs, and 133 fixed interface modes. The loaded modes used in the following sections are computed within the basis spanned by the fixed interface modes. This is clearly an approximation but has a marginal impact the results shown here. All pre-/post-processing and computations are performed using the SDT [12].

The reference elastic stiffness K_0 is built by combining the elastic model of the building and a layer of ground springs whose values is found by taking in each translation direction, the mean of the real part of the soil impedance at 1 Hz (approximately $2.5e9N/m$). K_d^{-1} is taken to be the inverse of K_0.

3.2 Selecting dynamic interface modes

In this first section, one seeks to demonstrate the validity of interface selection methods. To do so, one compares four cases.

The reduction basis for **model FI** combines fixed interface modes and a variable number of modes of the model condensed on soil/structure interface. Keeping all the interface modes would be equivalent to using the Craig-Bampton method [13]. Note that these modes can be approximated by building a mass matrix defined on the interface only, which may be more efficient numerically than condensing the model.

The reduction for basis for **model LO** keeps modes of the model associated with the reference stiffness K_0 and thus corresponds to a loaded interface CMS method. The drawback of this method is that there no longer is a decoupling between internal and interface deformations. This might be inefficient for a structure with many internal resonances.

For both model FI and LO, one compares a base version and a version where the static response $[K_0]^{-1}[b]$ to the spatial distribution of loads linked to the incoming waves computed at the low end of the frequency range. Keeping the real and imaginary parts for the three types of waves, leads to adding six interface modes. Better strategies for building a static

correction are considered in section 3.3.

Figures 2 and 3 show the strain energy error (6). The value shown is the maximum error for 15 frequencies between 1 and 15 Hz and 3 loading cases: *sv*, *sh* and *p* with vertical incidences.

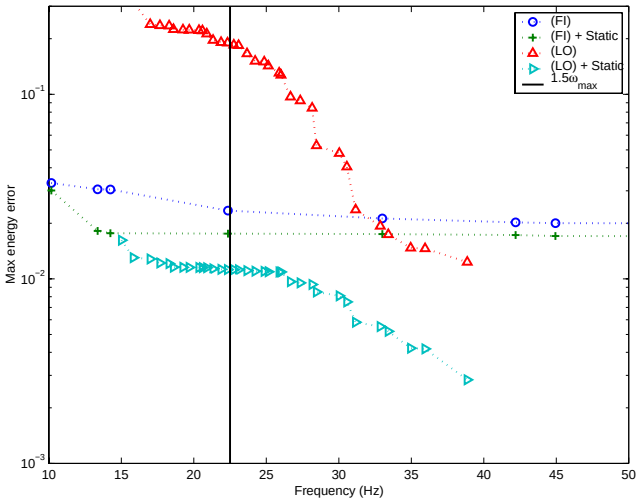

Figure 2: Maximum of energy error (6) as a function of frequency of last retained mode.

Figure 2 shows that for the standard threshold of $1.5\omega_{\max}$ (generally attributed to Rubin), model FI with no static correction gives reasonable results (3% max error). Including the static correction leads to somewhat better results. For model LO, the inclusion of a static correction drastically improves results.

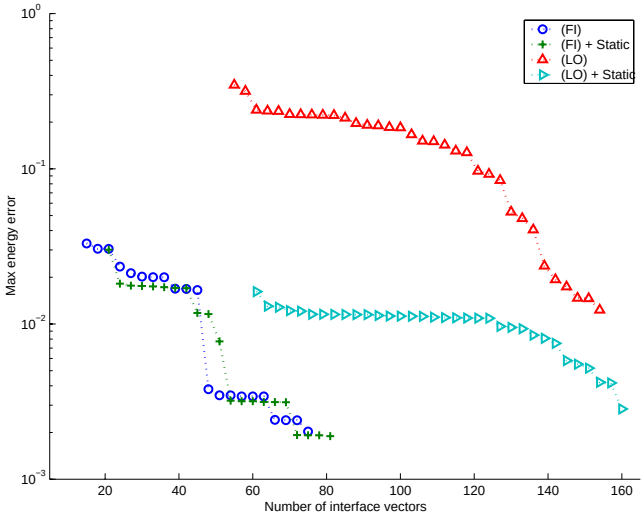

Figure 3: Maximum of energy error (6) as a function of number of modes with non zero displacement on interface (model FI has an additional 133 fixed interface modes)

Figure 3 gives a different perspective on the results by counting the number of interface modes. Starting values for kept modes are based on keeping all modes below the maximum frequency of interest. Model FI now seems to give better answers. This is due to the fact that the 133 fixed interface modes (modes below 30 Hz) are not counted since they are not used in soil impedance computations.

It clearly comes out that the best choice will depend on the relative cost of evaluating the soil impedance using the BEM method and evaluating the response. The use of static correction terms, for the spatial distribution of the inputs, is a very useful safeguard and should not be omitted. The use of the $1.5\omega_{\max}$ threshold is safe if such static correction is included.

Convergence often shows long series of modes with little variations. Evaluating the error by comparing a nominal model and a somewhat richer (where a number of additional interface modes have been included) can thus give very misleading results. Areas of slow convergence is a typical property of CMS methods and only iterations based on error estimation, illustrated in section 3.4, can change that.

3.3 Selecting input shapes for static correction

An important specificity of seismic loads is that the spatial distribution of loads varies with frequency. Doing a proper static correction, thus requires an appropriate treatment of these variations.

The simple approach, used in section 3.2, is to take the loads at a restricted number of frequencies

$$[b_I] = [\mathrm{Re}F_I(\omega_1)\ \mathrm{Im}F_I(\omega_1)\ \ldots\ \mathrm{Im}F_I(\omega_n)] \quad (11)$$

and include the static correction $K_d^{-1}b_I$ in the interface basis (typically after orthonormalization).

Based on the discussion in section 2.3, a first extension is to take a fairly large number of frequencies to build b_I, compute the singular value decomposition of these loads, and keep the vectors associated with the largest singular values. The SVD can be applied to b_I or to $K_d^{-1}b_I$. Figure 4 shows that SVD slopes obtained when considering each wave type separately or simultaneously is almost the same so that this is an open choice. When considering a large number of loading cases (3 wave types and 7 incidences), the global slope of the singular values is obviously smaller but the number of vectors found for a threshold of 10^{-2} or 10^{-3} is still quite small.

One should also note that singular values of $K_d^{-1}b_I$ fall much more rapidly than those of b_I this il-

lustrates the smoothing effect of computing the static response. In terms of convergence for the final model (shown in figure 5), doing the SVD on either gives similar results.

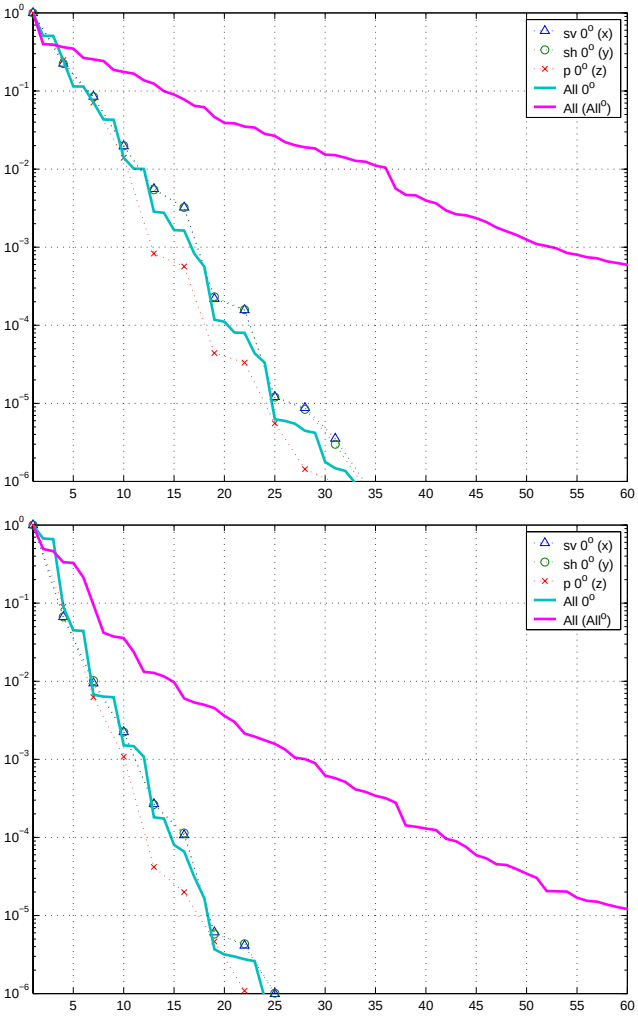

Figure 4: Singular values of the decomposition of $[b_I]$ (top) and $\left[K_d^{-1}\right][b_I]$ (bottom) for SV waves at 0^o, SH at 0^o, P at 0^o, all waves at 0^o, all waves at 7 different incidences

In practice, computing the singular value decomposition might rapidly become impractical if one is to compute the response at a large number of frequencies. An iterative method is thus introduced. An interface load basis is initialized with $b_I^{(1)} = [\mathrm{Re}\,(F_I(\omega_1))\ \mathrm{Im}\,(F_I(\omega_1))]$. One then loops on all loads at all frequencies and keeps those whose distance to their projection on the span of b_I^n is above a given tolerance. Thus, b_I^n is completed if

$$\frac{\left\|\left\{\hat{b}\right\} - [b_I^n]\left[b_I^{nT} b_I^n\right]^{-1}[b_I^n]^T\left\{\hat{b}\right\}\right\|}{\left\|\left\{\hat{b}\right\}\right\|} \leq \mathrm{Tol} \qquad (12)$$

for $\left\{\hat{b}\right\} = \mathrm{Re}\,(F_I(\omega_k))$ or $\left\{\hat{b}\right\} = \mathrm{Im}\,(F_I(\omega_k))$.

Again, the algorithm can also be applied on the static responses to the loads $\left[K_d^{-1}\right][F]$ rather that the loads themselves.

Figure 5 shows a comparison of results obtained with the proposed static mode selection schemes and a standard CB model with interface modes up to 15 Hz retained (see section 3.2). It appears that in this case, introducing static correction is indeed important, but even the most basic approach (keeping loads at the two frequency extremes) is sufficient.

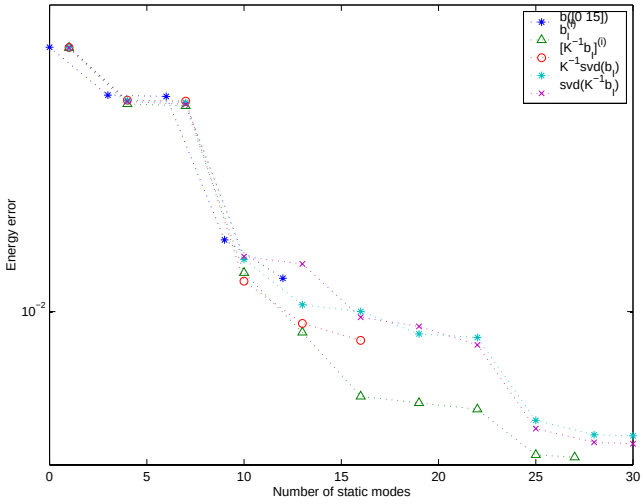

Figure 5: Evolution of maximum energy error, as a function of number of modes kept, for of various static mode selection schemes.

In practice, the iterative method (12) seems a good speed/accuracy compromise although scanning through the frequency interval would only be important if the medium modeled by the BEM can show resonant behavior.

3.4 Automated iterative methods

This section analyses results obtained with an iterative method based on the principles given in section 2.2. The reduction basis T_i is initialized using model LO with static correction considered in section 3.2. This corresponds to first point of figure 7, with 62 vectors retained and a maximum energy error at 2% for 3 wave types and 15 points between 1 and 15 Hz (figure 8 shows that for the sv wave used here the maximum energy error is below 1%). For enriching the basis, the tolerance on the strain energy error is set to 0.1%.

Figures 6 and 7 show two vertical frequency response functions at the top and bottom of the building respectively. The responses computed without basis enrichment show that a 2% maximum energy error does not correspond to a very accurate prediction of the FRF.

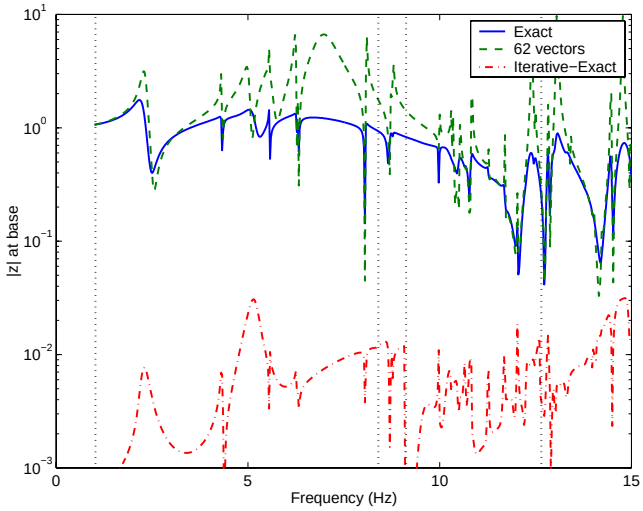

Figure 6: Frequency response at a vertical DOF of the base for sv wave loading at vertical incidence. Note that the iterative is so accurate that the amplitude of the difference is shown.

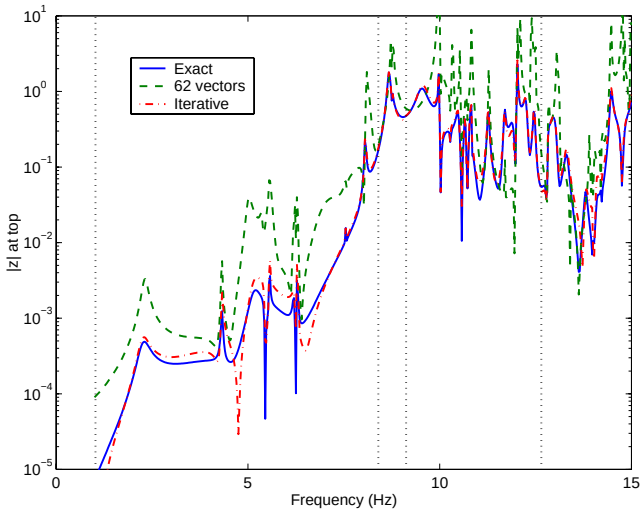

Figure 7: Frequency response at a vertical DOF the top of building for sv wave loading at vertical incidence.

The successive completion of the basis (shown as vertical dotted lines) lead to an almost exact response at the base of the building and a major improvement at the top. Thus with only 8 additional vectors an extremely accurate prediction of this very complex response is obtained.

Figure 8 shows the evolution of the error during the iterations. The steps are linked to the choice, which will be motivated later, not to evaluate errors at all frequencies. The error clearly shows a peak near the first mode but is otherwise difficult to relate to the evolution of errors on the FRFs. The iterative method does however significantly lower the energy error.

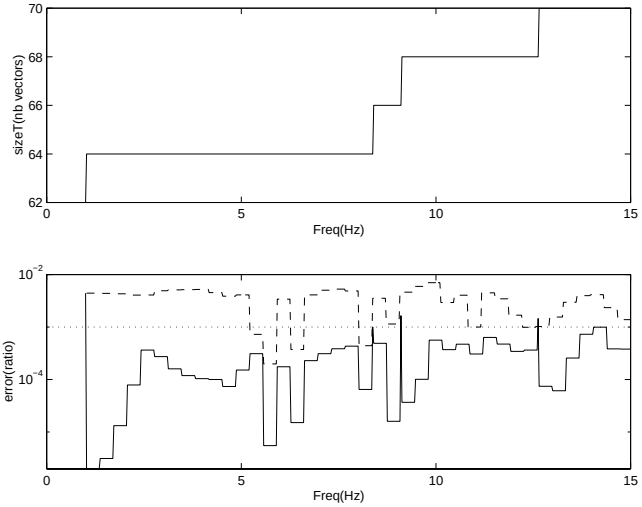

Figure 8: Evolution during iterations of basis size and energy error (– –) initial error with 62 vectors, (—) final result.

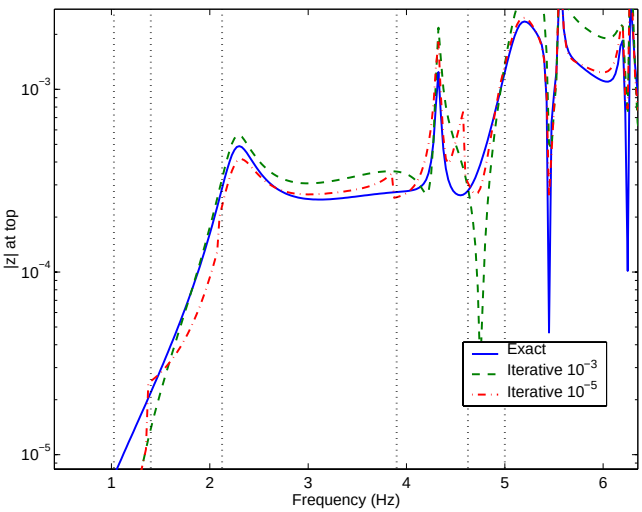

Figure 9: Frequency response at a vertical DOF the top of building for sv wave loading at vertical incidence. Exact and iterative methods with tolerance set to 10^{-3} and 10^{-5}

In order to gain a better understanding of the problems with the FRF at the top, one compared predictions obtained with the tolerance on strain energy error set at 10^{-3} and 10^{-5}. The results shown in figure 9 clearly indicate that better results are obtained

with the lower threshold. The projections on enriched bases, shown as vertical lines, however clearly induce breaks in the response. Fine tuning of the exact procedure used to enrich and compute a final prediction of the response is thus clearly needed.

Table 1 shows a number of time and memory evaluations that were considered to gain an understanding of the performance of the proposed methods. Times shown are CPU times on a SGI R10000 processor. Not all steps were equally optimized so that some caution should be used when interpreting results.

Table 1: Performance evaluations of full (558 interface DOF, 691 total) and reduced (70 generalized coordinates) approaches. Results shown for 100 frequencies except for time of projection.

Model	full	reduced
Computing Z_{soil}, F_I	1700 s	300 s
Loading Z_{soil}, F_I	540 s	65 s
Memory for Z_{soil}	475 MB	7 MB
Computing FRF	1087 s	2 s
Estimating R_D	–	28 s
Projecting model (per proj.)	–	21 s

Full interface computations are significantly dominated by the evaluation of the soil impedance and loading. If, as here, the coupled response is to be computed outside the BEM code, even reloading the soil matrices from a binary file represents a significant time and memory requirement.

When using reduced interface models, impedance computations and loading are somewhat faster (a factor of 20), whereas the cost of FRF computations becomes marginal. Since FRF computation is dominated by the inversion of the dynamic stiffness and full matrices are used, the speed-up should be of the order of the ratio of the dimensions cubed $(691/70)^3 \approx 1000$. The results found are actually not far from that.

The *a posteriori* estimation of energy error, which is necessary to assure the validity of predictions, and projecting the model when the need for refinement is detected, now become the dominant aspect of FRF evaluations. The strategy retained here is to evaluate the error at a fixed interval and backtrack to the last acceptable frequency point if an unacceptable level is detected. This technique was shown in figure 9 to induce some non-physical jumps in the response so that adaptations are needed.

4. Conclusion

The study has shown how CMS methods with interface model reduction procedures can be applied to build numerically efficient algorithms for coupled FEM/BEM predictions. The retained procedure combines *a priori* basis selection based on variations of traditional CMS procedures, and basis enrichment by an exact evaluation of error at a restricted set of frequencies.

It was found somewhat difficult to relate accuracy on FRFs and strain energy error thresholds. So further work on how to really measure the error is clearly needed. But a CPU time speedup of 7 and a reduction of memory requirements of 70 were obtained so that pursuing the work is clearly worthwhile.

In the last version of the algorithm, BEM computations take most of the time. Building BEM impedance approximation methods as proposed in Refs. [14, 15] would clearly be a useful complement to the present study. Finally, the overall procedure is also very useful in other applications where there are parametric variations of a nominal model (see [16] for example).

Acknowledgements

This work was partially supported by EDF under contract EP 970 “Fourniture de la version 1.0 du logiciel PROMISS 3D sous A.Q.”

References

[1] R. J. Craig, “A review of time-domain and frequency domain component mode synthesis methods,” *Int. J. Anal. and Exp. Modal Analysis*, vol. 2, no. 2, pp. 59–72, 1987.

[2] R. Craig and C. Chang, “Substructure coupling for dynamic analysis and testing,” *NASA CR-2781*, 1977.

[3] F. Bourquin and F. D’Hennezel, “Numerical study of an intrinsic component mode synthesis method,” *Rapport de recherche, INRIA No1329*, 1990.

[4] E. Balmès, “Use of generalized interface degrees of freedom in component mode synthesis,” *IMAC*, pp. 204–210, 1996.

[5] C. Farhat and M. Géradin, "On the general solution by a direct method of a large-scale singular system of linear equations: Application to the analysis of floating structures," *International Journal for Numerical Methods in Engineering*, vol. 41, pp. 675–696, 1998.

[6] E. Balmès, "De l'utilisation de la norme en énergie pour la création de modèles réduits en dynamique des structures," *C. R. Acad. Sci. , Paris, 323, Série IIb*, pp. 255–260, 1996.

[7] E. Balmès, "Optimal ritz vectors for component mode synthesis using the singular value decomposition," *AIAA Journal*, vol. 34, no. 6, pp. 1256–1260, 1996.

[8] D. Aubry and D. Clouteau, "A regularized boundary element method for stratified media," in *Mathematical and numerical aspects of wave propagation phenomena, Proc. 1st Int. Conf., Strasbourg, France, 23-26 April 1991* (G. Cohen, L. Halpern, and P. Joly, eds.), (SIAM, Philadelphia), pp. 660–668, INRIA, SIAM, 1991.

[9] D. Clouteau, *Propagation d'ondes dans des milieux hétérogènes, Application à la tenue d'ouvrages sous séismes*. PhD thesis, Ecole Centrale de Paris, 1990.

[10] D. Aubry and D. Clouteau, "A subdomain approach to dynamic soil-structure interaction," in *Recent advances in earthquake engineering and structural dynamics* (V. Davidovici and R. Clough, eds.), pp. 251–272, Nantes: Ouest Editions/AFPS, 1992.

[11] G. Devesa, "Opérateurs code_aster lire_miss_3d impr_miss_3d : documentation d'utilisation code_aster," Tech. Rep. U4.78.01 et U4.28.01, EDF/DER, 1998.

[12] E. Balmès, *Structural Dynamics Toolbox 4.0 (for use with MATLAB)*. International Technologies, http://www.sdtools.com, 2000.

[13] R. J. Craig and M. Bampton, "Coupling of substructures for dynamic analyses," *AIAA Journal*, vol. 6, no. 7, pp. 1313–1319, 1968.

[14] D. Schenk and B. G.W., "Structural acoustic coupling," *In Boundary Element Methods in Acoustics, Computational Mechanics Publications, R.D. Ciskowski, C.A. Brebia (eds.) Elsvier Applied Science*, 1991.

[15] J. Coyette, L. C., and M. J.L., "Calculations of vibro-acoustic frequency response functions using a single frequency boundary element solution and a padé expansion," *Acustica*, vol. 85, pp. 371–377, 1999.

[16] A. Plouin and E. Balmès, "Steel/viscoelastic/steel sandwich shells. computational methods and experimental validations.," *IMAC*, pp. 384–390, 200.